HIGH ORDER SPH-ALE METHOD FOR HYDRAULIC TURBINE SIMULATIONS

G-A. Renaut, S. Aubert, J-C. Marongiu

LMFA UMR CNRS 5509, Ecole centrale de Lyon, Ecully, France, gilles-alexis.renaut@ec-lyon.fr

LMFA UMR CNRS 5509, Ecole centrale de Lyon, Ecully, France, stephane.aubert@ec-lyon.fr

ANDRITZ Hydro SAS, Villeurbanne, France, jean-christophe.marongiu@andritz.com

ABSTRACT

This paper describes the development of a high order meshless method for the simulation of inviscid, weakly compressible, smooth and subsonic flows. The novelty of this approach is based on the use of least squares fitting to compute the state at the interface in the numerical flux reconstruction step. The main motivation of this work is to reduce the numerical dissipation in the Riemann solver used to compute inviscid fluxes. A second aspect of this paper is to develop an adaptive p-refinement in the frame of the SPH-ALE scheme i.e to adapt the order of this reconstruction. Numerical simulations show the accuracy and the robustness of the numerical approach for hydraulic turbines.

NOMENCLATURE

c_0 numerical speed sound [m/s]
C_p pressure coefficient
d number of dimension in space
D domain of influence of particle
G numerical flux
h smoothing length or dilatation parameter of one particle [m]
H Hessian matrix
i index of the particle of interest
j index of the neighbor of the particle i in D_i
J weighted square residual
M Least squares matrix. $M = QR$ with Q orthonormal and R upper triangular matrices
n_{ij} unit vector connecting the particles i and j oriented from i to j
p order of the polynomial reconstruction
P relative static pressure
$\wp$ polynomial basis for the least square reconstruction
t time [s]
v_0 transport field [m/s]
W_{ij} kernel function evaluated for particles i and j [m^{-3}]
$X = (X_{,1}, \cdots, X_{,d})$ vector position in $\Re^d$
X_{ij} position of the mid-point between the particles i and j
α limiter
ϵ_{app} reconstruction error estimator (reference value is 10^{-4})
∇ gradient operator

ω measure of the volume of particle $[m^3]$
ϕ state value of one particle
ϕ^h approximation of the state value ϕ
ρ density of fluid $[kg/m^3]$ (reference value $\rho_0 = 1000kg/m^3$)

INTRODUCTION

Nowadays computational fluid dynamics (CFD) is routinely used for many applications in aerodynamics, hydromechanics and aerospace. Complex geometries are discretized by unstructured grids. Mesh based methods like high order continuous finite element methods (FEMs), discontinuous Galerkin methods (DGMs) and finite volume methods (FVMs) have gained popularity for the numerical simulation of compressible and incompressible Euler and Navier-Stokes equations. For reasons of robustness and calculation cost, second-order schemes are routinely used for engineering problems. However, for a set of industrial applications, mesh-based methods are not always efficient and easy to use (free surface, moving geometries...).
In 1977, the meshless SPH method (Smoothed Particle Hydrodynamics) was proposed by Lucy for astrophysical applications. Later, the SPH-ALE method was developed by Vila (1999). The main idea of this variant of the SPH is to use Riemann solvers to compute numerical flux unlike classical SPH approach where an artificial viscosity is used to stabilize the method (Monaghan,1985).
The key issue in the development of high-order SPH-ALE schemes is the implementation of efficient reconstruction procedures of unknown variables at interface for each interaction. Indeed, the numerical dissipation due to the Riemann solver can be reduced with a MUSCL reconstruction (Monotone Upwind Scheme for Conservation Laws) introduced for finite volume method by van Leer (1979). The idea is to replace the piecewise constant approximation of Godunov's scheme by piecewise linear reconstructed states. One can extend this approach with higher orders ($p > 2$). It is called a p-refinement. Another way to increase the accuracy of the results and to reduce the numerical dissipation is to use particles that have a size gradually reduced. It is a h-refinement where h represents the particle size. In the finite element method, Babuska (1992) develops the idea to use both h and p refinements. A comparison between h and p refinements is presented in Li et al (2010) and shows the possibility of a p-refinement for smooth flows.
To obtain high order approximations in the frame of mesh-based method, and especially on unstructured meshes the k-exact method is widely used (Haider, 2013), (Barth, 1993). The Moving Least Squares method very famous in the meshless community is not really far from the k-exact method. The main difference lies in defining moments in the least squares matrix and in the iterative aspect of the k-exact method. The MLS method proposed by Lancaster and Salkauskas (1981) is used for smoothing and interpolating scattered data. Indeed it is often used in the field of meshless methods (Shobeyri et al, 2010) and in the field of unstructured Finite Volume (Chassaing, 2013). It is worth to notice that other alternative approaches were developed e.g. a hybridization between WENO (Weighted Essentially Non-Oscillatory) methods and MLS approximation was published to improve the accuracy of the SPH-ALE method for compressible flow (Avesani, 2014).
In the present work, a moving least square reconstruction using the recursive aspect of the k-exact method is used to show the ability of the p-refinement for the SPH-ALE method. The results of the p-refinement are compared with results obtained with the h-refinement. The rest of the paper is organized as follows. The governing equations and the SPH-ALE method are introduced in the next section. In a following section, the least squares reconstruction is exposed. The last section contains the numerical results where the proposed method is applied to inviscid weakly compressible flow for different types of particles' motion. Finally, some conclusions, remarks and an outlook to future research are given.

GOVERNING EQUATIONS AND SPH-ALE METHOD

The SPH-ALE method is based on a distribution of moving particles. The displacement of this set of particles is a regular vector field v_0. At time t, the particles coordinates are $X_i(t)$ and their volumes are $\omega_i(t)$. The following PDE in conservative form (Vila, 1999), (Vila and Lanson, 2008) is considered to model the time evolution of each particle position, volume and flow values:

$$\begin{cases} \frac{dX_i}{dt} = v_{0i}, \\ \\ \frac{d\omega_i}{dt} = \omega_i \sum_{j \in D_i} \omega_j (v_{0j} - v_{0i}) \nabla_i W_{ij}, \\ \\ \frac{d(\omega_i \phi_i)}{dt} + \omega_i \sum_{j \in D_i} \omega_j 2G(\phi_i, \phi_j, v_{0i}, v_{0j}, n_{ij}) \nabla_i W_{ij} = \omega_i S_i \end{cases} \tag{1}$$

The inviscid numerical flux G between two interacting particles i and j is composed of an eulerian numerical flux F along the n_{ij} direction and an ALE term where v_{0ij} and ϕ_{ij} are respectively the transport velocity and the state at the interface: $G(\phi_i, \phi_j, v_{0i}, v_{0j}, n_{ij}) = F(\phi_i, \phi_j, n_{ij}) - v_{0ij} \otimes \phi_{ij}$. The source term S could include gravity and viscosity effects. The sum over the neighborhood of i corresponds to the discrete computation of the divergence operator in the SPH framework. The SPH-ALE method can be seen as a cell-centered ALE Godunov-type method. Indeed, two specificities of this method can be developed :

1. The numerical flux G at each interface is computed from a moving Riemann problem formulated at the middle-point between particles' positions X_{ij}. This flux analogous to a finite volume flux includes a numerical viscosity. To increase the accuracy, $G(\phi_i, \phi_j, v_{0i}, v_{0j}, n_{ij})$ is replaced by $G(\phi_{ij}, \phi_{ji}, v_{0i}, v_{0j}, n_{ij})$ where ϕ_{ij} is an approximation of ϕ at X_{ij} given by a Taylor expansion from the point X_i.

2. This meshless method is connected with the notion of Arbitrary Lagrange Euler approximation. Indeed the value of the transport field v_0 can be imposed independently of the flow velocity . If this field is set to zero, particles have an Eulerian motion. If the transport field is equal to the flow velocity field, particles have a Lagrangian motion. Finally, if an arbitrary continuous transport field is imposed, they are in an ALE motion.

For more details about the SPH-ALE method, the reader is referred to the paper of Vila (1999).

HIGH ORDER RECONSTRUCTION FOR SCATTERED DATA

The Taylor expansion corresponding to a quadratic (p=2) reconstruction is given as :

$$\phi_i^h(X) = \phi_i + \nabla_i^T \phi (X - X_i) + \frac{1}{2}(X - X_i)^T H_i (X - X_i) \tag{2}$$

values $\nabla_i \phi$ and H_i are respectively the gradient and the Hessian matrix of the state variable ϕ evaluated at X_i. In the original paper of Vila (1999) this expansion used to evaluate the state at the interface involves a gradient computed with a SPH approximation based on a convolution product. It appears that in general the geometrical disorder of the particles' distribution is detrimental to the accuracy of this SPH approximation. Moreover the computation of derivative of order greater than 3 is complex. A central point in the development of higher-order methods (higher than second order) is a higher-order polynomial reconstruction of primitive variables ϕ within the control volumes. To achieve this, the MLS approach is based on a weighted least squares approximation over the neighboring data (Lancaster ,1981). These unknowns $\nabla_i \phi$ and H_i are found by minimizing per particle the sum of weighted squared residuals defined by :

$$J_i = \frac{1}{2} \sum_{j \in D_i} \omega_j W_{ij} [\phi_j - \phi_i^h(X_j)]^2 \tag{3}$$

The weighing function is $\omega_j W_{ij}$, where W_{ij} is the SPH kernel function centered on particle i. It has the isotropic compact support D_i and it is evaluated for every neighbors of the particle i in D_i. D_i defines the stencil of the least square fitting. These weight functions are often represented as function of the distance between two particles. In the present work, a Wendland function C4 is used. More details about the impact of the choice of those kernel functions are given in Khelladi (2011).

An algebraic system $MA = B$ appears when the equation Eq 3 is derived and written in a matrix form. The vector A contains the unknowns $\nabla_i\phi$ and H_i. The least squares matrix is $M = C^T W(X) C$ and the right hand side vector is $B = C^T W(X)\Delta\phi$. The vector $\Delta\phi$ is composed of differences of state between interacting particles i.e. $\phi_j - \phi_i$. The matrix M is symmetric and positive. The rows of the matrix C correspond to the development in the polynomial basis $\wp$ for each neighbors. For a 2D problem and an order of polynomial basis p, the basis is specified as : $\wp = [X_{,1}, X_{,2}]^T$ for $p = 1$ and $\wp = [X_{,1}, X_{,2}, X_{,1}^2, X_{,1}X_{,2}, X_{,2}^2]^T$ for $p = 2$. In order to preserve good numerical properties of the matrix M, a scaled centered basis is used : $(X - X_i)/h_i$ (Randles ,1997).

For example in a 2D case, the least square matrix for a linear reconstruction is given as :

$$M_{2,2} = \begin{pmatrix} \sum_{j\in D_i} \omega_j W_{ij} (\frac{X_{j,1}-X_{i,1}}{h_i})^2 & \sum_{j\in D_i} \omega_j W_{ij} (\frac{X_{j,1}-X_{i,1}}{h_i})(\frac{X_{j,2}-X_{i,2}}{h_i}) \\ \sum_{j\in D_i} \omega_j W_{ij} (\frac{X_{j,1}-X_{i,1}}{h_i})(\frac{X_{j,2}-X_{i,2}}{h_i}) & \sum_{j\in D_i} \omega_j W_{ij} (\frac{X_{j,2}-X_{i,2}}{h_i})^2 \end{pmatrix} \tag{4}$$

Numerical experience shows some geometrical configurations where it is impossible to solve the algebraic problem because the matrix M becomes ill-conditioned. For example, the representation of a quadratic polynomial basis in a truncated region is complicated by the lack of neighbors. To avoid this problem, a recursive algorithm of least square reconstruction was created by Barth (1993) and extended by Haider (2013). The k-derivatives are computed from the previous $k-1$ derivatives. A derivative of order two can be interpreted as two successive derivatives of order one. The advantage is to solve smaller algebraic problems per particle respectively 2×2 and 3×3 for 2D and 3D problems. Furthermore, the least squares matrix corresponding to a linear approximation is less sensitive to geometrical configuration.

To complete the MUSCL approach a limitation of the derivatives is introduced. Currently, there are many and various limitation techniques developed in mesh-based methods. A classical tool very close to unstructured finite volume inspired by Barth-Jespersen (1989) or Venkatakrishnan (1993) is used to avoid spurious oscillations. A parameter $\alpha_i \in [0; 1]$ is computed to limit the extrapolation of the field ϕ for the particle i and Eq 2 becomes :

$$\phi_i^h(X) = \phi_i + \alpha_i[\nabla_i^T \phi(X - X_i) + \frac{1}{2}(X - X_i)^T H_i (X - X_i)] \tag{5}$$

Numerical aspects :

In the frame of moving particles interacting with rotating solid, a robust and accurate technique of reconstruction is necessary whatever the geometric configuration is. Adaptivity and stability need to be discussed. On the other hand, as already mentioned in the introduction, there are two ways to reduce numerical dissipation : the first one is h-refinement and the second is p-refinement.

h-refinement

The h-refinement consists in reducing the particles size, what leads to decrease the size of the dilation parameter h and to increase the number of particles. The distance between nodal values being reduced, state discontinuities are weaker what reduces numerical viscosity. However this refinement increases drastically the computational cost. Besides, the time step size decreases because of the CFL condition that applies to explicit time integrators.

p-refinement : adaptivity in p-order and in d-space

Numerical robustness of this refinement method is closely connected to the number of nearby particles. The stencil is given by the compact support of the kernel function. It must be large enough to avoid an ill-conditioned matrix M. For a pth order polynomial basis, the number of neighbor particles must be higher than $(p+1)(p+2)/2$ and $(p+1)(p+2)(p+3)/6$ respectively in 2D and 3D. If those numbers are not satisfied, p must be decreased, until $p = 0$ sometimes. To strengthen the stability of the method, the d-adaptivity was implemented to handle various geometrical configurations of neighborhood of particles (Liu, 2003). For example, a set of points primarily aligned along the x-axis cannot give information about the derivatives along the y and z-axis. A polynomial basis of adjustable dimension is selected through a QR decomposition of the matrix M, where $M = QR$. Indeed, the orthogonal dense matrix Q contains the vector of the basis ($Q^TQ = I$). The coefficients of the upper triangular matrix R can be seen as a decomposition of the matrix M in the basis Q. In the case where a diagonal term of R is too small the matrix M cannot be fully decomposed in this basis. In the case of aligned particles in 2D, the smallest of the diagonal terms is half of the other. The idea behind d-adaptivity in this case is to project the least squares problem in the remaining 1D basis. The gradient in the other orthogonal direction is set to zero.

The concept of the p-adaptivity is to use high-order only when it is necessary, to reduce the cost of simulation without reducing the accuracy. To use adaptive p-refinement, a local approximation error is formulated by the least-squares functional evaluation (Perazzo 2008). This a posteriori error estimator is computed as : $\epsilon_{app} = ||\phi_j - \phi_i^h(X_j)||_{L_2(D_i)}/||\phi_j||_{L_2(D_i)}$. It is intuitively clear that the region where this indicator is high requires an increase of the reconstruction order, i.e adaptation. For example, a quadratic reconstruction (p=2) is necessary close to a leading edge of a solid body where gradients are stiff. The notations are in the following section "$p = 1$" and "$p = 2$" are for linear and quadratic approximation respectively. The possibility to have local linear or quadratic approximations in the same simulation depending on the local value of ϵ_{app} is noted "$p = 1$ *or* 2".

NUMERICAL RESULTS

In the following, the advantage of the p-refinement will be demonstrated in the case of an inviscid flow around a static symmetric NACA 0020 hydrofoil without incidence in 2D. Next, the robustness of the method for dynamic simulation is analyzed for a flow around two moving NACA 0020 hydrofoils. This test case shows the capacities of the p-refinement on a moving particles distribution for an unsteady flow. Indeed the particles distribution adapts itself to the motion of solid boundaries in an ALE manner (Neuhauser, 2014). The third test case corresponds to an industrial simulation of a water jet impacting rotating Pelton buckets in 3D. This last test case is computed to assess the method for more complex configurations (free surface, high dynamics on rotating geometry). For all three configurations, an explicit third order Runge-Kutta time integrator is used and the maximum of p-refinement is fixed equal to 2. The Euler equations are used to model the flow. The system is closed with a barotropic equation of the state to compute the relative pressure (Murnaghan, 1944): $P(\rho) = \frac{c_0^2\rho_0}{\gamma}[(\frac{\rho}{\rho_0})^\gamma - 1]$ where c_0 is the numerical sound speed, γ is taken equal to 7 and ρ_0 is the reference density ($\rho_0 = 1000kg/m^3$). The speed of sound is conveniently reduced to obtain a larger computational time step. It is chosen as $c_0 = 10U_{max}$ where U_{max} is the maximum expected fluid velocity.

Static NACA hydrofoil

This test case is computed with two objectives in mind. The first one is to assess the advantages of p-refinement over h-refinement. The second is to stress the robustness of the method of reconstruction

near the truncation of the computational domain due to the hydrofoil. The numerical Mach number is $0,1$ with a velocity at inlet $2\ m/s$. The chord of the hydrofoil is equal to one meter and its thickness is 20 $\%$ of chord. A refinement study is performed using a sequence of three distributions of points : $N, 2N, 4N$, i.e. respectively particles radius in $\{0,02; 0,0141; 0,01\}$ m. The distribution of points is obtained using the particle packing algorithm developed by Colagrossi (2012). The particles' motion is Eulerian. The coarse distribution corresponds to $N \approx 69000$ particles with 50 particles along the chord (Fig: 1b). The two finest distributions are obtained by refinement by $\sqrt{2}$ and 2 the particles radius. The farfield is situated 3 chords away from the leading and trailing edges. The velocity is imposed at the inlet and the pressure at the outlet. The top and bottom boundaries are periodic. The channel height is 6 m. The zero origin is at the middle of the chord.

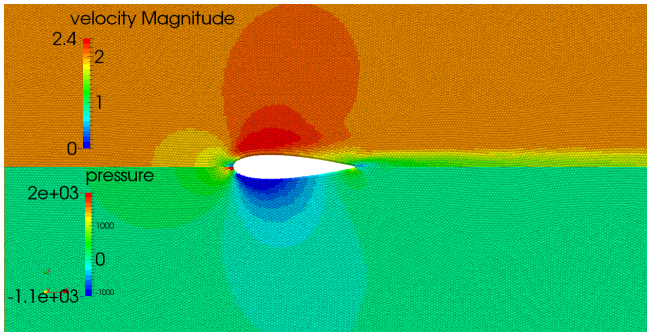

(a) Velocity and pressure fields for N particles and p=1

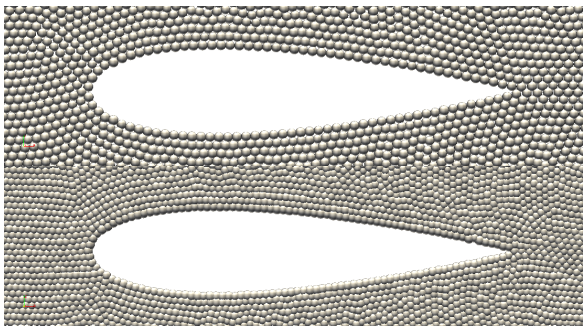

(b) Focus for N (top) and 2N (bottom) particles

Figure 1: Results for a steady flow around a static hydrofoil in (a) and distribution of particles in (b).

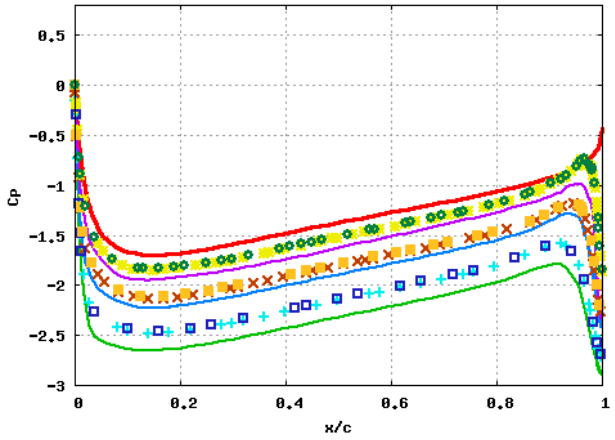

(a) Pressure coefficient along the hydrofoil wall

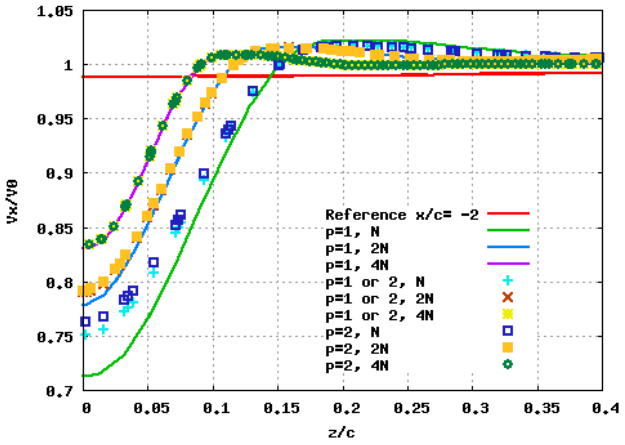

(b) Numerical wake behind the hydrofoil at x/c =2 in the cross-flow direction

Figure 2: Results for a static hydrofoil : symbols are presented in (b) and are identical in (a) and (b).

As it can be seen a significant numerical wake is formed behind the foil. For an inviscid flow it is due to the numerical viscosity. Its length can be seen on Fig: 1a. Fig: 2b presents a velocity profile along one line situated downstream at $x/c = +2$. The velocity profile along the line situated upstream at $x/c = -2$ is the reference. The numerical wake is reduced by the introduction of h-refinement (N,2N,4N labels) and/or p-refinement (p=1,p=2,p=1 or 2 labels). The pressure coefficient C_p along the hydrofoil presented in Fig 2a, is computed as: $C_p = \frac{P - P_{stag}}{\frac{1}{2}\rho U_\infty^2}$ where P_{stag} is the pressure at the stagnation point and U_∞ is the velocity imposed at inlet. Results are compared with

the potential solution computed with the freeware Xfoil (web.mit.edu/drela/Public/web/xfoil) for an isolated profile. It is to notice that the periodicity condition imposed on the top and bottom boundaries confines the flow between two adjacent blades. The resulting acceleration contributes to decrease C_p values compared to the isolated profile configuration. An improvement of the pressure coefficient with h and/or p refinement can be observed. The results converge to the potential solution. Adaptive p-refinement and full p-refinement shows very close results. The unphysical decrease of the C_p value at the trailing edge can be explained by a feature of the SPH method. Indeed the numerical stencil extends in this region over the two sides of the hydrofoil and introduces artificial connectivities across solid boundary. This aspect is not investigated in the present work.

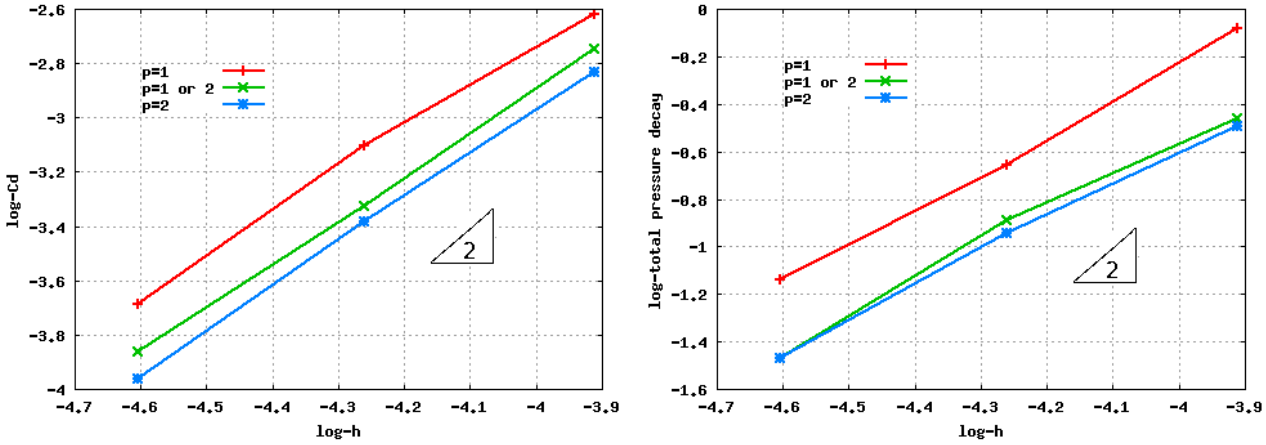

(a) Numerical drag coefficient for the hydrofoil

(b) Numerical total pressure decay for the hydrofoil

Figure 3: Results for a steady flow around a static hydrofoil for different orders of approximation.

The drag coefficient C_d and the total pressure decay between the inlet and the outlet are presented in Fig: 3a and 3b respectively. Drag coefficient is computed as: $C_d = \frac{F_x}{\frac{1}{2}\rho S U_\infty^2}$ where F_x represents the hydraulic forces along the flow axis. Total pressure decay is computed $\frac{P_{tot,outlet} - P_{tot,inlet}}{P_{tot,inlet}} \times 100$ where $P_{tot,inlet}$ is total pressure at inlet and $P_{tot,outlet}$ at outlet. Drag coefficient and total pressure should be zero for an inviscid flow; other values are directly connected to numerical dissipation. With refinements, numerical dissipation decreases and solutions are more accurate. It can be observed same slope equal to 2 for all type of reconstructions. This can be explained by the properties of the discrete divergence operator used in Eq 1. This operator is computed from the following continuous kernel approximation (expressed for a particle far of boundaries) :

$$\nabla.F(x) = \int_{D_i} \nabla F(y) W(x-y) dy = \int_{D_i} F(y) \nabla W(x-y) dy \tag{6}$$

Introducing the Taylor expansion of F it can be shown that a symmetric and positive kernel leads to second order $O(h^2)$ approximation (Monaghan, 1985). Moreover the ratio Dx/h connects the particle size Dx with the length ratio h. This ratio is often takes equal to 1.2. It can be concluded that the order of the numerical scheme of the SPH-ALE method is bounded by 2 without any improvement of the divergence operator approximation. A similar behavior is observed in the finite volume method where it is necessary to add quadrature points to increase the accuracy of the flux summation and obtain effective high order schemes (Delanaye, 1996).

Computational times to obtain one iteration and one physical second are compared Tab 1. p-refinement (p=2) increases by 36 $\%$ the cost. A h-refinement by a factor of $\sqrt{2}$ increases by $\sqrt{2}^3$ in

2D the cost to achieve one physical second. The number of points multiplied by two and the CFL condition explain this observation. Accordingly, p-refinement is much less expensive. p-adaptivity ($p = 1\ or\ 2$) manages to reduce the computational cost compared to full p-refinement (by about 15%) but it is slightly more dissipative. An overall of h and p refinements gives the best results (p=2 and 4N) on physical fields.

	p=1			**p=1 or 2**			**p=2**		
	N	**2N**	**4N**	**N**	**2N**	**4N**	**N**	**2N**	**4N**
CPU cost/iteration	*1,00*	1,99	4,00	1,19	2,33	4,81	1,36	2,70	5,44
CPU cost/second	*1,00*	2,81	8,01	1,19	3,29	9,63	1,36	3,81	10,87

Table 1: CPU time cost for h and p refinement (reference : p=1 ,N)

Dynamic NACA hydrofoils: Startup of a Francis turbine

At startup of a Francis turbine, guide vanes open to allow water to enter the machine. This key moment is modeled in the following test case in two dimensions (see Fig:4a). Water flows from left to right with an incidence of 7 degrees at inlet. The left hydrofoil models one opening guide vane and the right one represents one runner blade. They are separated by one chord. The guide vane opens from fully closed to fully opened in 20s with a smooth opening velocity. A cross-flow translation which mimics rotation is imposed to the runner blade $(0, 1m/s)$. After 20s the guide vane is steady, without incidence compared to the incoming flow. Blades dimensions are the same as in the previous test case. The particles radius is 2 cm corresponding to $N \approx 17000$ particles per channel. The farfield is situated 2.5 and 1.5 chords away from the leading edge of the first hydrofoil and the trailing edge of the second hydrofoil respectively. The total pressure is imposed at the inlet and the pressure at the outlet. A Periodicity is assumed in the cross-flow direction. The height of the domain is equal to the chord length, so that at initial time adjacent guide vanes are in contact, closing completely the channels.

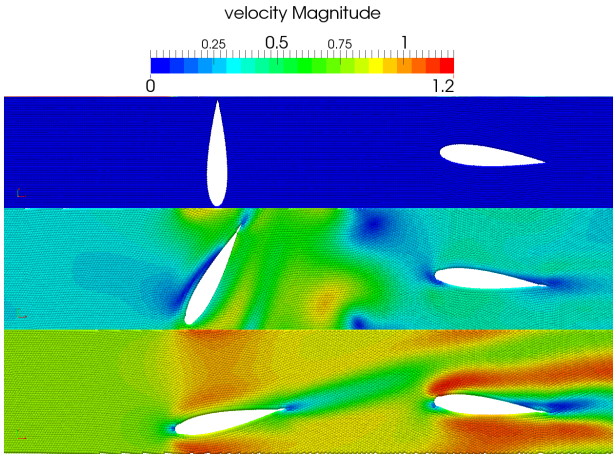

(a) Velocity field at t= 0s (top), 10s (middle), 20s (bottom)

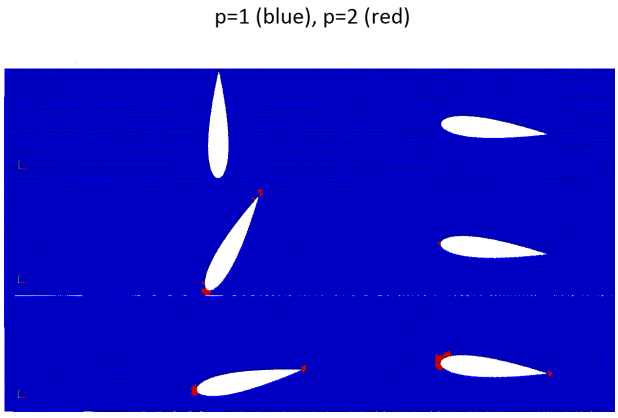

(b) p-adaptivity at t= 0s (top), 10s (middle), 20s (bottom)

Figure 4: Unsteady flow around moving hydrofoils

The velocity field is presented Fig 4a. At the initial time, the velocity field corresponds to a

velocity equal to $0\ m/s$ in the computational domain. At t=10s, the unsteady velocity field begins to become more intense by the opening of the blade runner. The final time presented (t=20s) shows a velocity field for a fully opened channel. In Fig 4b, p-adaptivity can be observed close to the leading and trailing edges where an adaptive higher order reconstruction is triggered (p=1 or 2). After 30s, the flow is stable and the guide vane is without incidence. Its drag coefficient for a linear approximation (p=1) is $Cd = 0,061$ for N particles. By doubling the particles number, the drag coefficient decreases to $C_d = 0,042$. With p-adaptivity, its value for N particles drops to $C_d = 0,05$ and $C_d = 0,045$ for full p-refinement (p=2). Again a reduction of numerical dissipation with p-refinement even with moving particles can be observed.

Pelton Turbine

This 3D test case is a simulation with a fully Lagrangian particles' motion of a Pelton turbine in operation. The rotating velocity of the buckets is imposed at 911 rpm and the velocity of the jet is $34m/s$ corresponding to a water height of 60 m. The particle size is 0,63 mm and the bucket width is 80 mm. There are 20 buckets, of which only 3 are simulated. The angular position of the first bucket is used to track the runner position.

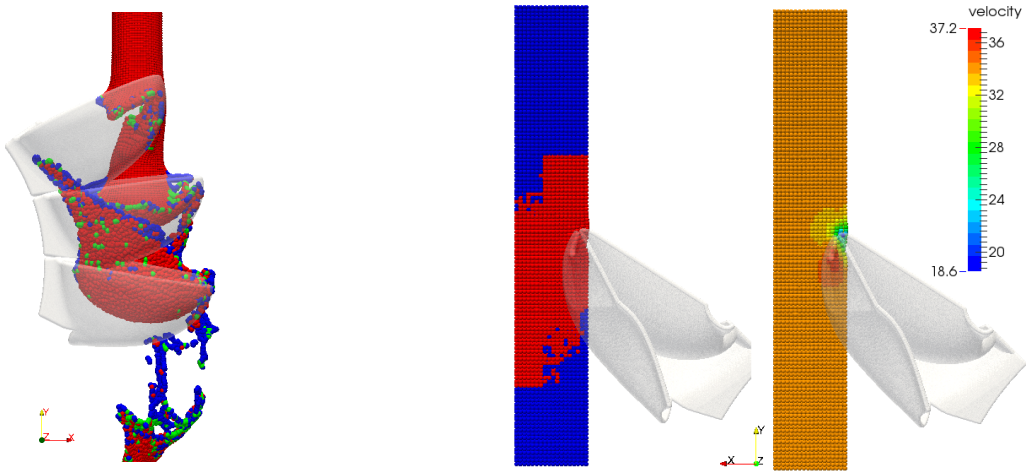

(a) Adaptivity in d-space at 114 degrees with p=1: d=1 (blue),2 (green), 3 (red)

(b) Adaptivity in p-order at 49 degrees: p=1 (blue); p=2 (red)

Figure 5: High velocity water jet impacting a rotating geometry of Pelton turbine in 3D

In Fig 5a, d-adaptivity is presented for a simulation with p=1 everywhere. It shows a side view of the water jet. The $M_{3\times3}$ is well defined for 95 % of the particles (in red). It is degenerated along one direction for 2 % of the particles (in green) and along two directions for 3 % of the particles (in blue). As expected, those 5 % are located in water sheets and fillets, where scattered and even isolated particles are predicted.

The figure 5b presents the moment where the entrance of the bucket nose in the water jet stiff gradients in the symmetry plan. As it can be seen the p-adaptivity adapts the order of reconstructions to the field. In Fig 6, numerical simulations are compared to experimental measurements at 2 probes on the rotating buckets. The local pressure coefficients are slightly improved by the p-refinement. Slopes and local extrema are closer to the experimental measurement. The p-refinement and the p-adaptivity give similar results because the high dynamics generate stiff gradients almost in the whole flow. During a simulation with p-refinement, the large majority of the particles use a quadratic reconstruction in 3D (93 %). The remaining particles use either constant reconstruction (isolated

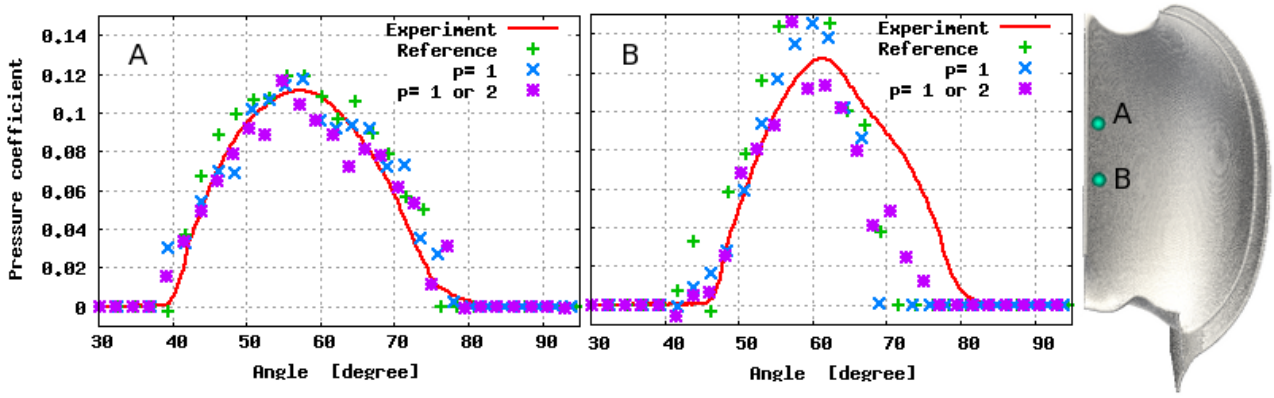

Figure 6: Pressure coefficient at two probes on rotating bucket wall (uncertainty of the pressure signals for experimental cases is 0.1%)

particles), or linear reconstruction (small number of neighbors) in all space dimensions with the d-adaptivity.

CONCLUSIONS

A new Least-Square-SPH-ALE method was proposed in the present work to increase the accuracy of the meshless simulations in multidimensions in space. The MLS formalism with the recursive aspect of the k-exact method was used to compute high order extrapolations. The results show that the method is able to produce accurate and stable results in simulating complex problems (free surface, flow around a solid). After focusing flux reconstructions, future work will focus on the flux summation approximating the divergence operator.

ACKNOWLEDGEMENTS

The first author is partly supported by the French government through the Association Nationale de la Recherche et de Technologie (CIFRE grant 2012/1620) and by ANDRITZ Hydro.

REFERENCES

D. Avesani and al, *A new class of moving-least-squares WENO-SPH schemes*,113-154,Journal of Computational Physics (2014), http://dx.doi.org/10.1016/j.jcp.2014.03.041.

I. Babuska, and B.Q .Guo *The h, p and h-p version of the finite element method: basis theory and applications*, Advances in Engineering Software,Volume 15, Issue 3-4, 1992.

T. Barth, *Recent developments in high order k-exact reconstruction on unstructured meshes.*, AIAA-93-0668, pp. 1-15., Reno Nevada 1993.

J.C. Chassaing, X. Nogueira and S. Khelladi, *Accuracy assessment of a high-order moving least squares finite volume method for compressible flows*, 71 pp 41-53 Comput. Fluids , 2013.

A. Colagrossi, B. Bouscasse, M. Antuono, S. Marrone,, *Particle packing algorithm for SPH schemes*, 113-154 Computer Physics Communications 183, 1641-1653, 2012.

J-M. Delanaye, *Polynomial reconstruction finite volume schemes for the compressible Euler and Navier-Stokes equations on unstrutured Adaptive grids* PhD thesis, University of Liege, Switzerland, 1996.

F. Haider,P. Brenner, B. Courbet and J.-P. Croisille *Parallel implementation of k-exact Finite Volume Reconstruction on Unstructured Grid*, HONOM, 12 june 2013.

A. Huerta, T. Belytscho, S. Fernandez-Mendez and T. Rabczuk, *Meshfree Methods*, Encyclopedia of Computational Mechanics , 2004.

A. Iske, L. Bonaventura, E. Miglio, *Kernel Based Vector Field Reconstruction in Computational Fuild Dynamic Model*,Int. J. Numer. Meth. Fluids 00:1-6 , 2000.

S. Khelladi, X. Nogueira, F. Bakir,I. Colominas *Toward a higher order unsteady finite volume solver based on reproducing kernel methods*, Compt Methods Appl.Mech Engrg,2348-2362, 2011.

P. Lancaster, K. Salkauskas, *Surfaces generated by moving least squares methods*, Mathematics of Computation, 87: 141-158, 1981.

Y. Li,S. Premasuthan and A. Jameson, *Comparison of h- and p- Adaptations for Spectral Difference Methods* , 40th Fluid Dynamics Conference and Exhibit,Chicago, AIAA 4435 ,2010.

G. R. Liu *Mesh free methods: moving beyond the finite element method*, 4th ed., Vols. 1 and 2, CRC Press, London, 2003.

J.J. Monaghan and H. Pongracic, *Artificial viscosity for particle methods*, Applied Numerical Mathematcis 1:187-194,1985.

F.D. Murnaghan, *The Compressibility of Media under Extreme Pressures*, Proceedings of the National Academy of Sciences of the United States of America, vol. 30 1944, p. 244-247.

M. Neuhauser *Development of a coupled SPH-ALE/Finite Volume method for the simulation of transient flows in hydraulic machines* PhD thesis in Ecole Centrale de Lyon, 2014 .

F. Perazzo , R. Lohner, L. Perez-Pozo, *Adaptive methodology for meshless finite point method* , Advances in Engineering Software 39 156-166, 2008.

G. Shobeyri and M.H. Afshar, *Simulating free surface problems using Discrete Least Squares Meshless method*, 113-154 Computers Fluids 39 461-470,2010.

J.P. Vila, *On particle weighted methods and Smooth particle hydrodynamics*, 3rd ed Mathematical Models and Methods in Applied Sciences, 1999.

V. Venkatakrishnan, *On the accuracy of limiters and convergence to steady solutions* , AIAA 93-0880 Computer Sciences Corporation,1993.